

Machine Learning Assisted Antenna Optimization with Data Augmentation

Jiapeng Zhang, Jiawen Xu, Qiang Chen and Hui Li, *Senior Member, IEEE*

Abstract—In this letter, a machine learning assisted antenna optimization method is proposed based on the random forest (RF) algorithm with data augmentation (DA). Using only a small number of samples, the prediction and optimization accuracy of the RF algorithm is ensured with repeated data augmentation, which balances different types of samples during the training. With the proposed DA-RF method, the AR bandwidth of a circularly polarized omnidirectional base station antenna is optimized. By learning the relationship between the loop orientations and the AR bandwidth efficiently, the AR bandwidth is improved by 41% compared with the best one in the samples. The estimation accuracy of the proposed method outperforms other similar methods, with fewer iterations as well. The method is also successfully applied to multi-objective optimizations.

Index Terms—Antenna optimization, base station antennas, data augmentation, circularly polarization, machine learning, random forest (RF).

I. INTRODUCTION

THE advancement of machine learning (ML) in electromagnetics (EM) provides new approaches for antenna design [1]-[4]. The framework of the ML-assisted antenna design is shown in Fig. 1, where the dataset is dynamically updated as the ML model learns. The ML model can replace part of the computationally intensive EM simulations, and make the antenna design procedure time efficient.

Different ML-based methods have been exploited to optimize the antennas. Dynamic graph convolutional neural networks (DGCNNs) [5] and artificial neural network (ANN) [6] have been utilized to predict the objective parameters of the antenna, though the predicted result deviates a bit from that using the EM simulators. A deep neural network (DNN) method can achieve reliable optimization using a huge number of randomly generated samples (e.g., 10^5 - 10^6 samples) [7]. However, larger number of samples indicate a considerable amount of time for EM simulations. In [8], a ML-based surrogate-assisted particle swarm optimization method can provide favorable results with a much smaller number of EM

This work was supported in part by (1) National natural science foundation of China (No. 61971087); (2) LiaoNing Revitalization Talents Program (No. XLYC1907074); (3) China Postdoctoral Science Foundation (No. 2019T120200 and No. 2018M631779). Jiapeng Zhang, Jiawen Xu and Hui Li are with School of Information and Communication Engineering, Dalian University of Technology, Dalian, 116024, China. Qiang Chen is with Research Institute of Electrical Communication, Tohoku University, 980-8577, Japan. (Corresponding author: Hui Li)

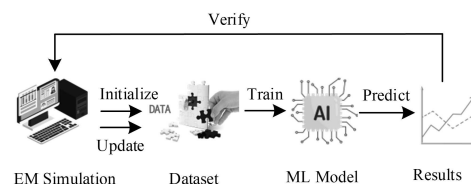


Fig. 1. Framework of the ML-assisted antenna design optimization.

simulations. In [9], an improved KNN method requires only 10-100 samples, with some prior knowledge during the learning process. An ANN method with 100 training data samples has also been used to optimize a Fabry-Perot (FP) resonator antenna with three geometrical variables [10].

Random forest (RF) is a supervised learning algorithm [11] for classification and regression [12], [13], with decision trees as the base learner. In [14], RF algorithm is used as a classifier to process multipath information and improve the performance of the time difference of arrival (TDOA) localization system. As a regression surrogate model in antenna design, the computational overhead of the RF is low, since the method is less affected by the size of the dataset [15]-[17]. RF can also predict multiple objectives, which are the real and imaginary parts of electric fields in [18]. For multi-objective optimization, ANN and Gaussian process regression (GPR) are efficient methods as well without requiring any new simulations [19].

In this letter, an improved method based on RF is proposed for antenna estimation, which requires a small number of samples and provides good prediction accuracy. Data augmentation (DA) based on sample classifications is carried out to balance the datasets and increase the prediction accuracy. The method is applied to a circularly polarized omnidirectional base station antenna, in order to achieve wider AR bandwidth, higher gain and better roundness. As a result, antenna performances have been improved by 90 MHz, 0.8 dBi and 0.33 dB during single-objective optimizations, compared with the best values in the samples.

II. DA-RF OPTIMIZATION METHOD

This section describes the DA-RF based method in predicting the optimal antenna parameters. The regression model of RF algorithm is employed, which consists of multiple regression trees. The final output of the model is jointly determined by all the decision trees in the forest, which is independent from each other.

The RF regressor is implemented according to the following steps:

- 1) Use Bootstrap to generate training subsets for each decision tree;
- 2) Randomly extract features for node splitting to establish decision trees, which are combined to form a random forest;
- 3) Average the outputs of all the decision trees, which is provided as the final output.

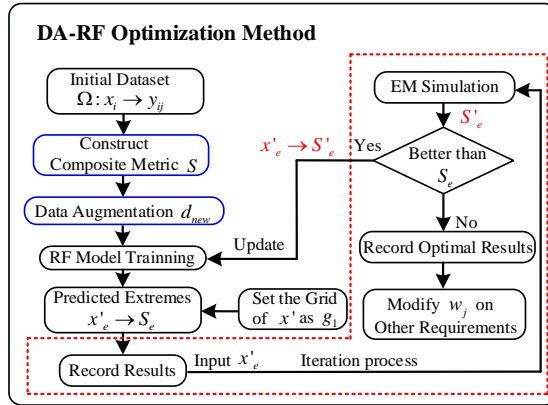


Fig. 2. The optimization process of the proposed DA-RF method.

The optimization process using the proposed DA-RF method is given in Fig. 2. Firstly, for an optimization with N objectives, antenna design parameters are put into the EM simulators to obtain a dataset $\Omega: x_i \rightarrow y_{ij} (j=1,2,\dots,N)$. Typically, the original dataset from the simulations is divided into a training set and a test set with the ratio of 9:1. Afterwards, the multiple objectives are weighted based on the statistical distribution of the samples, transforming the multi-objective issue to a single-objective problem. Since the few-shot learning could result in sample imbalance using different construction methods, data augmentation is introduced to improve the RF-based method. The augmented dataset is then trained using the RF model. Based on the training results, the antenna design parameters that lead to better target values are predicted on the refined grid g_l of the input x' . The predicted target value is denoted as S_e , with its corresponding design parameters denoted as x'_e .

Those design parameters are then simulated in the full-wave EM simulators for validation. If the simulated value S'_e is better than S_e , the training dataset is then updated with the new dataset, and the learning process is iterated. Otherwise, the optimization is terminated, and the optimal results are obtained. The critical procedures, including target reconstruction and data augmentation, are illustrated in details in the following subsections.

A. Construction of Composite Metric

For a multi-objective optimization, it is difficult to achieve optimal values for all the objectives at the same time. In order to simplify the multi-objective optimization, a composite metric S with weighted objectives is utilized:

$$S = \sum_{j=1}^N w_j y_j, \quad (1)$$

where w_j is the weighting coefficients for the j -th objective y_j . Compared with single-objective optimizations, the multi-objective optimization, when weighted together, faces the problem of different scales. To balance the contribution of different objectives, the weighting coefficient of the j -th objective is calculated from

$$w_j = \frac{\prod_{i=1}^N \sum_{i=1}^n \frac{1}{n} y_{ij}}{\sum_{i=1}^n \frac{1}{n} y_{ij}}, \quad (2)$$

where $\sum_{i=1}^n \frac{1}{n} y_{ij}$ is the averaged value of the j -th objective in the training dataset. The training process is then applied to learn the mapping relationship $\Omega^*: x_i \rightarrow S(w_j, y_j)$.

B. Data Augmentation

To obtain the initial dataset, uniform grid is adopted over the antenna design parameters, which is similar to conventional parameter sweepings in the EM simulators. A small number of samples would result in imbalanced dataset measured by the target. For example, there are much more samples with narrow bandwidth than those with large bandwidth. The imbalanced data in the training set prevents the algorithm from learning more essential features, resulting in unrobust model.

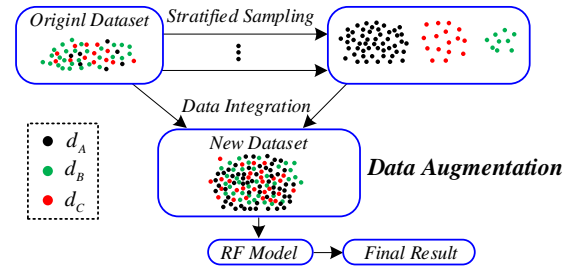


Fig. 3. Data augmentation for improving the accuracy of the RF-based method.

To balance the datasets, the training dataset d is classified into three groups based on the target values, i.e., good dataset d_A , medium dataset d_B and bad dataset d_C . Afterwards, data augmentation based on stratified oversampling is exploited to balance the number of the samples in different groups, as illustrated in Fig. 3. Different from the general oversampling that is applied to all the dataset with no differences, the stratified oversampling is carried out differently for different layers. If the number of data is small in one dataset, more samples are selected and added back, and vice versa. That is to say, the oversampling in different datasets is performed inversely proportional to the number of the data in that dataset. The oversampling procedure is repeated until the numbers of the data in different layers are almost the same, so that the features for different datasets can be well learned. Considering the time cost in the EM simulators, repeated samples, rather than new samples, in each group are re-used.

III. DESIGN EXAMPLE

In this section, a design example of a circularly polarized omnidirectional base station antenna is presented to illustrate the proposed DA-RF method. Both single-objective and multi-objective optimizations are carried out.

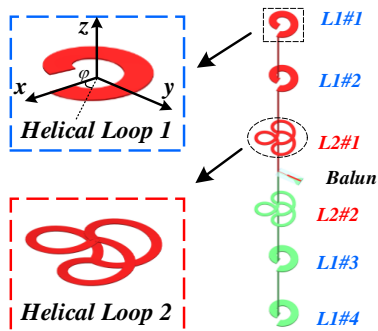


Fig. 4. Geometries of the circularly polarized omnidirectional base station antenna.

A. Antenna Configuration

The configuration of the six-stage circularly polarized omnidirectional base station antenna is presented in Fig. 4. It is composed of cascaded vertical strips and helical loops, fed by a tapered balun. The performance of the antenna is mainly limited by its AR bandwidth over all the horizontal angles, though it has been improved from the original design in [20] by replacing the center loops with parallel loops. The initial AR bandwidth of the based station antenna in Fig. 4 is 64 MHz when the four helical loops are in the same orientation as in the figure. Due to the asymmetrical structure of the antenna, the AR bandwidths at some certain horizontal angles are very small, which limit the overall bandwidth. With intuition, the open ends of the four loops are orientated uniformly to 0° , 90° , 180° and 270° , which enlarges the AR bandwidth to 112 MHz. We can assume that by arranging the orientations of the loops, an even larger AR bandwidth can be achieved. However, there are too many combinations among the rotations of the four loops. For example, if each loop has 36 possible rotation angles, there are 36^4 combinations in total, which makes parameter sweeping impossible. Hence, the DA-RF method is employed.

B. Single-objective optimization

The AR bandwidth is set as the optimization target. The rotation angles of the four loops on the xoy plane are set as the input variables, i.e., $x_i = [\varphi_1, \varphi_2, \varphi_3, \varphi_4]$. The definition of φ is denoted in Fig. 4, where 0° is along the x -axis. For each loop, a step width of 120° is chosen, resulting in 81 samples established by CST Microwave Studio [21]. The maximum AR bandwidth in the sample is 188 MHz, which corresponds to a relative bandwidth of 6.1%.

The datasets are then sorted according to their AR bandwidth. The top 10% samples in the bandwidth are considered as good datasets, whereas the ones with bandwidths smaller than 100 MHz are determined as bad datasets. The rest of the samples belong to the medium dataset. As a result of the classification, there are 8, 16 and 57 samples, respectively, in the good, medium and bad datasets, showing unbalanced samples with the ratio of around 1:2:8. According to the principle of the data

augmentation in section II-B, an inversely proportional ratio of 8:4:1 is used for stratified oversampling. After 7 times of oversampling, there are 64, 44 and 64 samples, respectively, in the good, medium and bad datasets, which are much more balanced. Subsequently, RF training is carried out based on those samples.

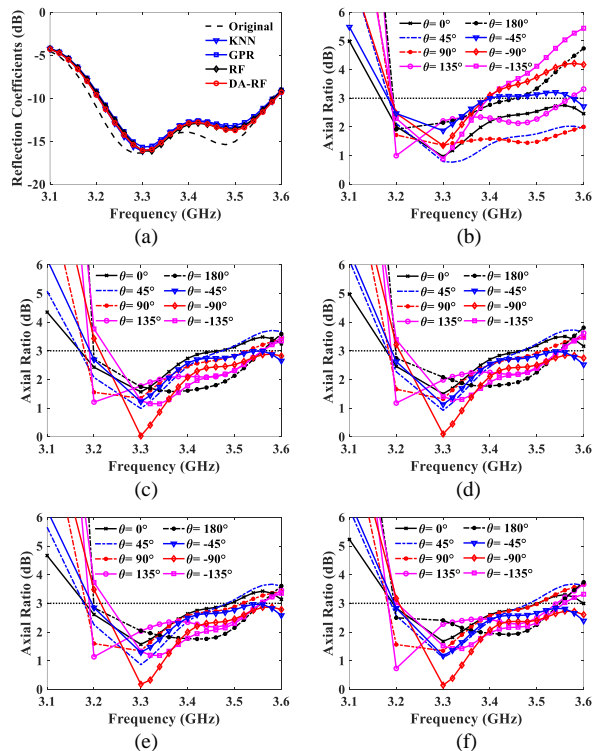


Fig. 5. Simulated performance of the circularly polarized omnidirectional base station antenna: (a) Reflection coefficients; (b) Best AR bandwidth in the samples; (c) Optimized AR bandwidth by KNN; (d) Optimized AR bandwidth by GPR; (e) Optimized AR bandwidth by conventional RF; (f) Optimized AR bandwidth by DA-RF.

During the prediction, the step width in grid g_1 is set to 10° . Following the procedure in Fig. 2, the optimization terminates after 24 iterations, providing the optimal AR bandwidth of 278 MHz. The corresponding input parameter is $x'_e = [230^\circ, 170^\circ, 200^\circ, 110^\circ]$. The optimization takes 52 minutes in total. To show the advantage of the proposed method, similar ML algorithms, including the KNN, GPR and conventional RF, are employed to optimize the AR bandwidth using the same initial dataset. The optimized AR bandwidths at different horizontal angles are given in Fig. 5(b)-(f) with a step width of 45° , which basically indicates their omnidirectional performances. The results are summarized and compared in Table I. The reflection coefficients in Fig. 5(a) show that the impedance bandwidth is always larger than the AR bandwidth. In other words, the AR bandwidth is the bottleneck of the antenna performances.

Among all the algorithms in Table I, KNN requires the least number of iterations. However, its optimized bandwidth is also the smallest, which is 44 MHz narrower than the one using the proposed method. Too many iterations are required for GPR, due to the small number of samples. In contrast, the proposed DA-RF method leads to the largest bandwidth with relatively fewer iterations and less execution time. The bandwidth has

been improved by 41% compared with the best one in the samples.

TABLE I
COMPARISON OF AR BANDWIDTH USING DIFFERENT METHODS

Method	Bandwidth (MHz)	Relative Bandwidth	Increment	Iteration	Execution Time (Min)
KNN	235	7.0%	14.8%	17	36
GPR	246	7.4%	21.3%	87	183
RF	253	7.6%	24.6%	33	69
DA-RF	279	8.6%	41.0%	24	52

As a second example of single-objective optimization, the maximum gain at 3.3 GHz is optimized, which follows the similar procedures to the AR bandwidth optimization. The results converge within 9 iterations, with an optimal design parameter x'_e of $[100^\circ, 160^\circ, 80^\circ, 140^\circ]$. The optimized gains are compared with the configuration with the maximum gain in the 81 samples in Table II. The maximum gain is improved to 9 dBi, which is 0.8 dB higher than the original one. The average gain over the operating band is enlarged as well.

C. Multi-objective optimization

For multi-objective optimization, the performances of the 81 initial samples, including the AR bandwidth, the realized gain and the pattern roundness, are investigated. All the three targets are taken into consideration using the composite metric illustrated in section II-B. According to (2), the weighting coefficients for the bandwidth, gain and roundness are 21.5, 275.4 and -691.4, respectively.

TABLE II
COMPARISON OF OPTIMIZATION RESULTS

	Bandwidth (MHz)	Relative Bandwidth	Gain (dBi)	Roundness (dB)	S
Sample	188	6.1%	7.32	2.59	3606
	96	2.3%	8.20	3.38	1650
	71	2.3%	6.68	1.03	1856
Single-Objective	278	8.6%	7.19	2.89	5210
	5	0.2%	9.00	4.19	-306
	68	2.1%	6.5	0.7	1903
Multi-Objective	290	8.6%	7.24	2.52	5588

The optimized results are provided in Table II. For each single optimization, the specific target has been greatly improved compared with the best one in the samples. For the multi-objective optimization, better results can be achieved. The optimal one with the largest S provides an AR bandwidth of 290 MHz, a realized gain of 7.24 dBi and a roundness of 2.52 dB. The antenna design parameters corresponding to the optimal S are $[250^\circ, 160^\circ, 180^\circ, 140^\circ]$, and the optimization converges within 32 iterations. The impedance bandwidth is always large enough to cover the AR bandwidth during the optimization. More balanced performances are achieved compared with the results of single-objective optimizations. Hence, the proposed method is effective and efficient in both single-objective and multi-objective optimizations of antennas parameters.

IV. ANTENNA EXPERIMENTS

To fabricate a robust metallic antenna, the thickness of the aluminum was changed to 1.8 mm, which was then re-optimized using the proposed DA-RF method. The largest AR

bandwidth of 198 MHz was achieved when the input parameter x'_e is $[230^\circ, 130^\circ, 180^\circ, 80^\circ]$, which improved by 31% compared with the best one in the samples [22]. According to the optimized configuration, the antenna was fabricated, with the prototype given in Fig. 6(a). The vertical strips and helical loops, which were made of aluminum alloy, were fabricated with all-metal 3-D printing. The balun is printed on the substrate of F4B, with the permittivity of 2.2 and loss tangent of 0.001.

The reflection coefficients of the antenna were measured using Ceyear-3672C vector network analyzer, with the results given in Fig. 7(a). The measured bandwidth was slightly larger than the simulated ones and moved to the lower frequencies, covering 3.13-3.48 GHz. The radiation performances of the proposed antenna in the operating band were measured in the SATIMO chamber, with the measurement setup given in Fig. 6(b). As shown in Fig. 7(b), the measured AR agreed well with the simulated ones in general. Similar to the reflection coefficients, the operating frequencies for the circular polarization also moved towards the lower band, which could be attributed to the fabrication tolerance of the 3-D printing and the material difference between the aluminum in the simulation and the aluminum alloy in the fabrication. The overlapped bandwidth in the measurement was from 3.15 to 3.41 GHz, which was around 260 MHz.

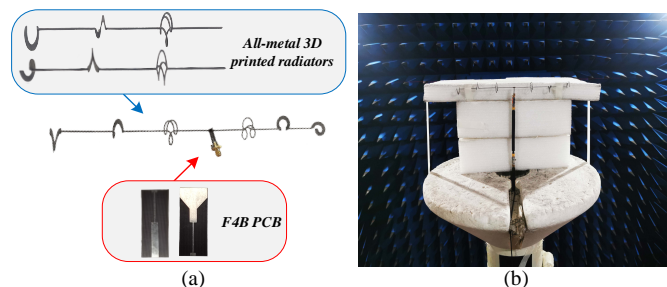


Fig. 6. (a) Fabricated antenna prototype; (b) Measurement setup of the optimized antenna.

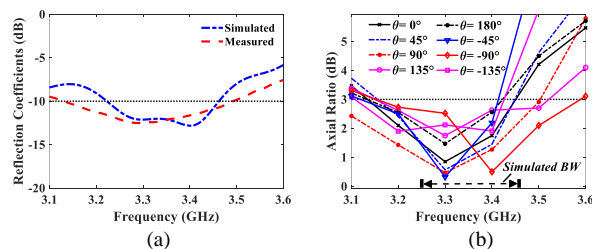


Fig. 7. Measured and simulated results of the circularly polarized omnidirectional base station antenna: (a) Reflection coefficients; (b) AR values.

V. CONCLUSION

In this letter, a DA-RF method is proposed to efficiently optimize the antenna parameters for specific targets. With DA, only a small number of samples are required for accurate prediction, which greatly reduces the simulation time. The method is applied to a circularly polarized base station antenna. As a result, the AR bandwidth has been improved from 188 MHz to 278 MHz. The DA-RF method outperforms other similar ML-based methods in terms of better prediction results and fewer iterations. The method has also been validated in multi-objective applications.

REFERENCES

- [1] Z. Bayraktar *et al.*, "Guest editorial: Special cluster on machine learning applications in electromagnetics, antennas, and propagation," *IEEE Trans. Antennas Propag.*, vol. 18, no. 11, pp. 2220-2224, Nov. 2019.
- [2] D. Erricolo *et al.*, "Machine learning in electromagnetics: a review and some perspectives for future research," in *Proc. of 2019 IEEE Int. Conf. Electromagn. Adv. Appl.*, Granada, Spain, 2019, pp. 1377-1380.
- [3] R. Haupt and P. Rocca, "Artificial intelligence in electromagnetics," *IEEE Trans. Antennas Propag. Mag.*, vol. 63, no. 3, p. 14, Jun. 2021.
- [4] S. K. Goudos *et al.*, "Guest editorial: special section on computational intelligence in antennas and propagation: emerging trends and applications," *IEEE Open J. Antennas Propag.*, vol. 2, pp. 224-229, 2021.
- [5] W. Xiang *et al.*, "Fast prediction of Quasi-Periodic array using dynamical graph convolutional neural networks," *IEEE Antennas Wireless Propag. Lett.*, vol. 21, no. 5, pp. 893-897, May. 2022.
- [6] E. Cil *et al.*, "Machine learning-based matching medium design for implant communications," *IEEE Trans. Antennas Propag.*, vol. 68, no. 10, pp. 5199-5208, Jul. 2022.
- [7] K. Z. Ž. Stanković, D. I. Olćan, N. S. Dončov and B. M. Kolundžija, "Consensus deep neural networks for antenna design and optimization," *IEEE Trans. Antennas Propag.*, vol. 70, no. 7, pp. 5015-5023, Jul. 2022.
- [8] K. Fu, X. Cai, B. Yuan, Y. Yang and X. Yao, "An efficient surrogate assisted particle swarm optimization for antenna synthesis," *IEEE Trans. Antennas Propag.*, vol. 70, no. 7, pp. 4977-4984, Jul. 2022.
- [9] E. Cil *et al.*, "A modified efficient KNN method for antenna optimization and design," *IEEE Trans. Antennas Propag.*, vol. 68, no. 10, pp. 6858-6866, Oct. 2020.
- [10] L.-Y. Xiao, W. Shao, F.-L. Jin, and B.-Z. Wang, "Multiparameter modeling with ANN for antenna design," *IEEE Trans. Antennas Propag.*, vol. 66, no. 7, pp. 3718-3723, Jul. 2018.
- [11] Breiman L, "Random forests," *Mach. Learning.*, vol. 45, no. 1, pp. 5-32, 2001.
- [12] Cutler A, Cutler D R, Stevens J R, "Random forests," *Ensemble Mach. Learning.* Springer, Boston, MA, pp. 157-175, 2012.
- [13] Criminisi A, Shotton J and Konukoglu E, "Decision forests for classification, regression, density estimation, manifold learning and semi-supervised learning," *Now Foundations and Trends.*, 2012.
- [14] M. N. de Sousa and R. S. Thomä, "Applying random forest and multipath fingerprints to enhance TDOA localization systems," *IEEE Antennas Wireless Propag. Lett.*, vol. 18, no. 11, pp. 2316-2320, Nov. 2019.
- [15] N. Kurniawati, D. Novita Nurmala Putri and Y. Kurnia Ningsih, "Random forest regression for predicting metamaterial antenna parameters," in *Proc. IEEE 2nd. Int. Conf. Ind. Elect. Electron.*, Lombok, Indonesia, 2020, pp. 174-178.
- [16] M. R. Khan, C. L. Zekios, S. Bhardwaj and S. V. Georgakopoulos, "Performance of random forest algorithm in high-dimensional surrogate modeling of antennas," in *Proc. IEEE Int. Symp. Antennas Propag. USNC-URSI Radio Sci. Meeting.*, Singapore, Singapore, 2021, pp. 1445-1446.
- [17] S. Pavithran, S. Viswasom, S. K. S and A. J, "Designing of a 5G multiband antenna using decision tree and random forest regression models," in *Proc. IEEE 8th. Int. Conf. Signal Process Integrated Networks.*, Noida, India, 2021, pp. 626-631.
- [18] Y. Zhao *et al.*, "Reconstruction of the statistical characteristics of electric fields in enclosures with an aperture based on random forest regression," *IEEE Trans. Electromagnet Compat.*, vol. 62, no. 4, pp. 1151-1159, Aug. 2020.
- [19] Y. Sharma *et al.* "Machine learning methods-based modeling and optimization of 3-D-Printed dielectrics around monopole antenna," *IEEE Trans. Antennas Propag.*, vol. 70, no. 7, pp. 4997-5006, Jul. 2022.
- [20] W. Lin and R. W. Ziolkowski, "Compact, high directivity, omnidirectional circularly polarized antenna array," *IEEE Trans. Antennas Propag.*, vol. 67, no. 7, pp. 4537-4547, Jul. 2019.
- [21] J. Zhang. (2022). *DA-RF*. [Online]. Available: <https://github.com/JP-Zhang0210/DA-RF/blob/main/Sample-81.txt>
- [22] J. Zhang. (2022). *DA-RF*. [Online]. Available: <https://github.com/JP-Zhang0210/DA-RF/blob/main/Sample-81-fm.txt>